Journal of Sound and Vibration (1979) **64**(3), 387–402

INTERPRETATION OF GAS OSCILLATIONS IN MULTICYLINDER FLUID MACHINERY MANIFOLDS BY USING LUMPED PARAMETER DESCRIPTIONS

R. SINGH† AND W. SOEDEL

Ray W. Herrick Laboratories, School of Mechanical Engineering, Purdue University, West Lafayette, Indiana 47907, *U.S.A.*

(*Received* 25 *April* 1977, *and in revised form* 15 *January* 1979)

Fluid pressure oscillations are complicated in multicylinder positive displacement machinery manifolds because of the cylinder interactions due to (i) the kinematic arrangements between cylinders and (ii) the inter-connected manifold elements. In practice, manifolds possess irregular shapes and geometries. These are difficult to analyze by using a continuous parameters approach; however, the manifold components can be discretized easily and described by acoustic lumped parameters. Additionally, this approach is more suitable for developing design guidelines, which is the primary aim of the present paper. The multicylinder interaction problem is formulated in the frequency domain. Mass flow rates, with proper crank phase relationships, are considered excitation sources. Manifold components are described as acoustic elements. The equations of acoustic motion are solved for the eigenvalues and the natural modes of gas oscillation, and these are used to provide the forced acoustic response. The formulations are then applied to a two-cylinder compressor discharge system. The computed results compare well with measurements.

1. INTRODUCTION

An insight into the nature of fluid pressure oscillations in the manifolds of positive displacement machinery is important because of their influence on thermodynamic performance, noise and vibration [1]. Manifold design guidelines for a single cylinder machine are generally understood. But, these cannot be readily extended to multicylinder machines because of the dynamic interactions between the cylinders.

1.1. LITERATURE REVIEW

The work in the area of modeling of multicylinder manifolds is very limited. Soedel *et al.* [2, 3] applied an acoustic lumped parameters approach to simulate two-cylinder refrigeration compressor discharge interactions. The discharge model was described in the time domain, and was coupled with the compressor process models. This technique was then extended to a four-cylinder automotive compressor discharge system [4]. It was also applied to a single cylinder two-stroke cycle chain saw engine, for which it was found necessary to include combustion chamber and muffler volume models in an overall multi-degree of freedom Helmholtz resonator model [5]. The results of these investigations produced good

† Now at Carlyle Compressor Company, Carrier Corporation, P.O. Box 4803, Syracuse, New York 13221, U.S.A.

0022–460X/79/110387 + 16 $02.00/0

agreements with experimental data and this has established the validity of lumped parameters modeling of the manifolds. Karnopp [6] has also utilized the lumped parameters approach for mufflers, and obtained solutions for these models by using the bond graph technique.

Schwerzler [7] modeled suction and discharge systems of a multiple-cylinder compressor by using only a quasi-steady mean pressure variation technique in which dynamic coupling effects between cylinders are ignored. Wang [8] also did not account for these interactions in his analysis of a multicylinder engine induction system. In this investigation, cylinders were considered in parallel, and only sequential time relationships between them were modeled. Benson and Ucer [9] also did not consider multicylinder interactions in their method of characteristics technique.

The authors [10, 11] have developed a modeling procedure in which multicylinder manifold components are described by their acoustic impedances in the distributed parameters format. A "building-block" type of transfer function approach is used to construct an overall mathematical model. It is coupled with time-variant compressor process models, and an iterative computational procedure is employed for the solution, which accounts for the back pressure effect. The authors have also developed an impedance measurement technique [12] to aid manifold mathematical modeling. Although the continuous system approach is potentially very accurate and powerful, it does not readily provide an insight into the physics of the problem. To obtain this, a less accurate approach (lumped parameters) is used here.

1.2. OBJECTIVES AND ASSUMPTIONS

The major aim of the work reported in this paper was to define and formulate multicylinder manifold problems in order to determine acoustic eigenvalues and the oscillating pressure response. These are important from the thermodynamic capacity and performance viewpoint as badly designed manifolds can increase energy requirements significantly. Also, large pressure variations can lead to pipeline vibrations, noise, failure, etc. Thus, the emphasis of the analysis here is more on the manifold design aspects and less on the precise computations of pressure pulsations.

A two-cylinder compressor discharge manifold will be analyzed by using acoustic theory [13, 14]. The assumptions are as follows.

(1) The pressure disturbances propagate as plane wave fronts. This assumption is justified as generally the lower frequency pulsations are dominant. Also, transverse dimensions of manifolds are often smaller than the shortest wavelength of interest. Moreover, in some previous investigations [2–8] this assumption has been verified.

(2) Manifold elements can be modeled as discretized acoustic elements. Stalzer and Fiedler [15] have examined the criteria for the validity of applying the lumped parameters approach to fluid transients, and report that this representation is sufficient for any fluid, except for very long lines or high frequencies. This assumption is attractive from the modeling viewpoint as complicated and irregular manifold cavities and passages can be easily analyzed. It is, however, at the expense of computation accuracy and an upper frequency limitation of the analysis. Shape factors such as those proposed by Alster [16] could be used to improve accuracy. In a number of previous investigations [2–5], good correlations between lumped parameters based theory and measurements have been obtained. Karnopp [6] has proposed a dual approach in which a continuous system could be described by a series of normal modes. This would extend the flexibility of the lumped parameters approach.

(3) The source is not affected by the manifold pressure response. In positive displacement machines, mass flow rate through ports is the source, and is certainly affected by the pressure variations in the manifolds. It is considered negligible for the sake of analysis simplicity: otherwise, a mathematical simulation of the whole machine would be required [7, 8]. An alternate approach could be to describe the source by an equivalent acoustic impedance.

(4) For the convenience of analysis, the manifold termination is considered to be either of zero or of infinite impedance. The omission of a realistic termination is not a serious limitation, in the context of this analysis. For instance, an anechoic termination can be taken care of by a judicious selection of damping. As another example, it was found for a two-cylinder case that the exit impedance did not affect the inner manifold response strongly. This was confirmed by measurements [2, 7–9] which show that in reciprocating compressors pressure oscillations are not as dominant in the exit pipe as in the inner cavities. For detailed analysis, realistic termination descriptions should of course be included [9].

(5) Convective effects of the mean fluid flow have been ignored. This assumption is justified as generally the Mach number in compressor suction and discharge lines is less than 0·1.

(6) The acoustic damping model is linear but incorporates an empirical coefficient, by means of which non-linear fluid flow effects can be accounted for (see section 2.3).

2. PROBLEM FORMULATION

2.1. MULTICYLINDER INTERACTIONS

One can picture the multicylinder manifold as a composite dynamic system with multiple periodic non-simultaneous inputs. The fluid-dynamic interactions can be thought of as resulting from two types of coupling: kinematic and geometric.

2.1.1. *Kinematic coupling*

The kinematic arrangement of a multicylinder reciprocating compressor is such that the instantaneous crank angle (θ_i) for a cylinder is

$$\theta_i = \omega t + \phi_i, \qquad i = 1, \ldots, m, \tag{1a}$$

$$\phi_1 = 0. \tag{1b}$$

Since the compressor operation is a cyclic phenomenon, all the processes in a particular cylinder will be ahead or behind those in the other cylinders by kinematic phase differences.

2.1.2. *Geometric coupling*

The cylinders are generally connected to each other through manifold passages and plenums. The mean fluid flow follows the pattern of these geometries and is pumped downstream. The acoustic waves not only propagate down the discharge line of one cylinder but also influence each other through the connecting elements. The impedance inequalities, all over the lines, would reflect the acoustic waves back. Thus, in a discharge plenum there are incident and reflected waves corresponding to not only its respective cylinder but also to all the other cylinders. Hence, the resulting pressure in front of any discharge valve has components corresponding to all of the mass flow rates. Of course, the main component is due to its own mass flow rate input, and other cylinders may enhance or subdue it. Similarly, at any other point in the system, the waves from all the cylinders interfere with each other.

Kinematic coupling in the absence of cavity coupling will not cause any dynamic interactions between the cylinders. The only result will be that the discharge pressures of all the cylinders will have the same phase relationships amongst them as that of the rest of the compressor processes. On the other hand, the cavity coupling in the absence of kinematic coupling will cause fluid-dynamic interactions. The waves, from all of the valve exits, will start simultaneously and propagate in the system, and interference will take place. When the kinematic coupling is superimposed on the cavity couplings, then the waves from the valve exits do not start simultaneously and the interference phenomenon is going to be rather complicated. One has to keep track of both the amplitude and phase of each and every harmonic of a cylinder. The in-phase harmonics cause a constructive interference and the out-of-phase harmonics cause a destructive interference.

2.2. EXCITATION

Soedel *et al.* [2] considered the mean fluid pressure differential to be the forcing function. The pressures were evaluated from the mass flow rates. Their forcing functions did not show any separate term for a kinematic arrangement, but the kinematic effect was built in as the cylinder thermodynamic and fluid flow equations were solved for each θ_i. Here, it is proposed to use mass flow rate through a discharge valve ($\dot{m}_v$) to be an input to the system, but not in the time domain, rather in the frequency domain. This concept has also been followed by the authors in their efforts with the distributed parameters modeling [10, 11]; ϕ is considered with $\dot{m}_v$. For the cylinder i, the mass flow $\dot{m}_{v_i}$ can be decomposed into Fourier components (a list of nomenclature is given in Appendix B),

$$\dot{m}_{v_i}(t)|_{\theta_i} = \left[\dot{m}_{v_i} + \sum_{n=1}^{N} \{|\dot{m}_{v_i}(n\omega)| \cos(n\omega t + \psi_{\dot{m}_i}(n\omega))\} \right]_{\theta_i}. \tag{2}$$

The input volume velocity $Q_i(n\omega)$ is

$$Q_i(n\omega)|_{\theta_i} = \dot{m}_{v_i}(n\omega)/\rho|_{\theta_i}, \tag{3}$$

where $Q_i(n\omega)$ is a complex number of magnitude $|Q_i(n\omega)|$ and phase $\psi_{Q_i}(n\omega)$. The gas density is ρ. Thus

$$Q_i(n\omega)|_{\theta_i} e^{j\omega t} = |Q_i(n\omega)| \cos(n\omega t + \psi_{Q_i}(n\omega))|_{\theta_i}. \tag{4}$$

To evaluate analytically the effect of kinematic phasing (ϕ_i) between cylinders on volume velocity harmonics, consider cylinders 1 and i. If both cylinders discharge an equal volume flow rate, say $Q(t)$, then

$$Q_1(t) = H(t)Q(t) \qquad \text{and} \qquad Q_i(t) = H\left(t - \frac{\phi_i}{\omega}\right) Q\left(t - \frac{\phi_i}{\omega}\right) \tag{5}$$

where $H(t)$ is the unit step function. The Laplace transform L gives

$$L\{Q_1(t)\} = Q(s) \qquad \text{and} \qquad L\{Q_i(t)\} = e^{(\phi_i/\omega)s} Q(s). \tag{6}$$

Thus the phase between two discharges in the Laplace domain is $(\phi_i/\omega)s$. Since the volume flow rate through the valves is a periodic phenomenon (of period $2\pi/\omega$), the Laplace domain can be converted into a Fourier domain by substituting $s = j n\omega$. Therefore, the nth harmonics of the two cylinders have $n\phi_i$ phase difference. For a case of m cylinders, the nth harmonics of the 2nd, 3rd, ..., mth cylinder lag the nth harmonic of the first cylinder by $n\phi_2, n\phi_3, \ldots, n\phi_m$. With this knowledge, the Fourier transforms for all mass flow rates can be computed on the same time or crank angle basis and then the phase relationships can be added to it.

2.3. LUMPED PARAMETERS REPRESENTATION

For the application of the lumped parameters theory, it is essential to recognize the different acoustic elements.

2.3.1. *Acoustic mass M*

The inertial element can be considered as an incompressible fluid plug which moves as a unit. The element opposes a change in the volume velocity, and is of value

$$M = \rho l/S. \tag{7}$$

It should be noted that l is the effective acoustic length which includes end corrections [13, 14].

2.3.2. *Acoustic stiffness K*

A volume can be modeled as an elastic element because the gas contained within is considered to be compressible. The pressure inside changes as it is alternately compressed and expanded by the influx and efflux of the fluid through the opening.

The form of the volume is immaterial. However, the largest dimension of the shape should conform to the restriction imposed by the shortest wavelength of interest [13, 14]. The acoustic stiffness K for a cavity of volume V is

$$K = \rho c^2/V. \tag{8}$$

2.3.3. *Acoustic damping R*

The attenuation of small amplitude plane acoustic waves in a fluid at rest contained in a tube with rigid walls, due to the viscous and heat conduction losses at the boundary, is well understood and can be predicted theoretically. In the presence of mean fluid flow, however, and with higher acoustic amplitudes, additional losses can occur [14]. These may be due to the finite amplitudes and/or acoustic/mean flow interaction. In high speed refrigeration compressor (positive displacement type) manifolds, the situation is further complicated by the following: (a) the flow medium is always laden with lubricating oil vapors, it is often not possible to assess oil circulation rates precisely, and thus the prediction of thermodynamic properties is difficult, and (b) one often encounters irregular orifice-like elements, such as connecting passages, in the manifolds; these may exhibit large dissipation characteristics. Because of the complexity of the nature of flow-induced damping and availability of mathematical models (most of which have been developed with air as the medium [14]), experimental means must be adopted to assess the damping values [17] (see Appendix A).

For modeling purposes, however, the frictional force per unit area can be assumed to be proportional to $\dot{X}$, and the proportionality constant, called the acoustic damping R, will account for the overall damping including the above mentioned non-linear effects, as shown in Appendix A. Thus, this non-linear phenomenon is being treated by a linear model where R is independent of $\dot{X}$. Here, R will be associated with an inertial element M,

$$R = R_M M, \tag{9a}$$

where, from equation (A7),

$$R_M = \zeta \sqrt{2\pi\mu\omega/\rho S} \tag{9b}$$

where ζ is a non-dimensional fluid-induced damping coefficient [17].

In practical manifolds, one often finds irregular shapes and geometries. For analysis purposes, the manifold components can be classified in the following manner: (i) the necks, passages and orifices are generally inertial and resistance elements, and (ii) the cavities and plenums possess only elastic properties.

2.4. ACOUSTIC RESPONSE

The equations of acoustic motion can be developed in the following matrix form (see reference [18] for some example cases):

$$[M]\{\ddot{X}(t)\} + [R]\{\dot{X}(t)\} + [K]\{X(t)\} = \{F(t)\}. \tag{10}$$

As the volume displacements $\dot{X}(t)$ are associated with the acoustic masses and resistances, the mass $[M]$ and damping $[R]$ matrices are diagonal. The forcing function vector includes the input volume velocity terms. Equation (10) could be solved either in the time domain by using a Runge–Kutta procedure or in the frequency domain by using a harmonic solution approach, which is followed here.

The eigenvalue solution of equation (10) provides natural frequencies (ω_r) and modes of oscillation (u_r). The displacement solution can be obtained by using the modal expansion approach [19]:

$$\{X(t)\} = \sum_{r=1} \{u\}_r h_r(t), \tag{11a}$$

where

$$h_r(t) = \frac{1}{\delta_r} \int_0^t N_r(t)\, e^{-\eta_r(t-\tau)} \sin \delta_r(t-\tau)\, d\tau, \tag{11b}$$

$$N_r(t) = \{u\}_r^T\{F\}/\{u\}_r^T[M]\{u\}_r, \qquad \eta_r = \xi_r \omega_r, \tag{11c,d}$$

$$\delta_r = \omega_r\sqrt{1-\xi_r^2}, \qquad \xi_r = R_M/2\omega_r. \tag{11e,f}$$

For a tube of unit length and cross-sectional area S,

$$\xi_r = (\zeta_r/\omega_r)\sqrt{\pi\mu\omega/2\rho S}. \tag{11g}$$

Note that equation (11a) contains only the forced solution as the transient solution (corresponding to the initial conditions) is not of practical interest.

3. EXAMPLE CASE

The theory, developed in the last section, will now be applied to a two-cylinder case. The schematic of a discharge system is shown in Figure 1. The mechanical and electrical analogs of the discharge system dynamics are presented in Figure 2.

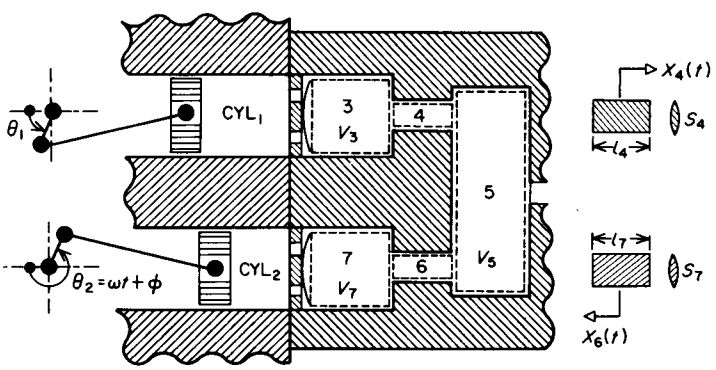

Figure 1. Discharge manifold schematic for a two-cylinder compressor.

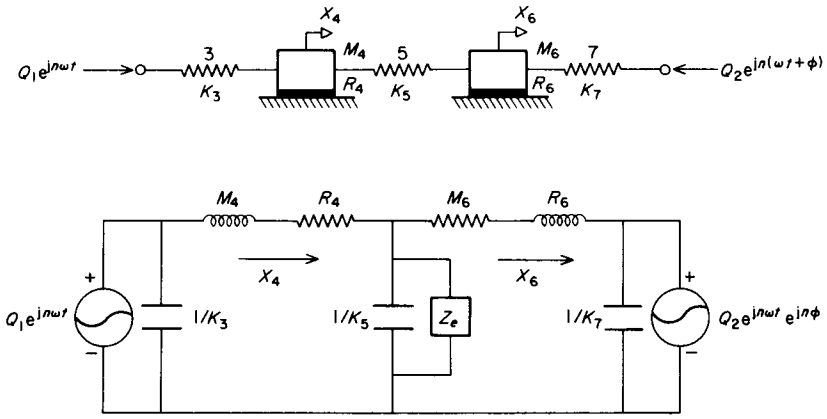

Figure 2. Mechanical and electrical analogs of the discharge manifold shown in Figure 5.

3.1. EQUATIONS OF MOTION AND EIGENVALUE SOLUTION

For the discharge system depicted in Figure 1, the matrices for the equation of motion (10) are

$$[M] = \begin{bmatrix} M_4 & 0 \\ 0 & M_6 \end{bmatrix} = \rho \begin{bmatrix} l_4/S_4 & 0 \\ 0 & l_6/S_6 \end{bmatrix}, \qquad [R] = \begin{bmatrix} R_4 & 0 \\ 0 & R_6 \end{bmatrix}, \tag{12a,b}$$

$$[K] = \begin{bmatrix} K_3 + K_5 & -K_5 \\ -K_5 & K_5 + K_7 \end{bmatrix} = \rho c^2 \begin{bmatrix} (1/V_3) + (1/V_5) & -1/V_5 \\ -1/V_5 & (1/V_5) + (1/V_7) \end{bmatrix}, \tag{12c}$$

$$\{X(t)\} = \begin{Bmatrix} X_4(t) \\ X_6(t) \end{Bmatrix}, \tag{12d}$$

$$\{F(t)\} = \begin{Bmatrix} F_1(t) \\ F_2(t) \end{Bmatrix} e^{jn\omega t} = \begin{Bmatrix} +(K_3/jn\omega)Q_1 \\ -(K_7/jn\omega)Q_2\, e^{jn\phi} \end{Bmatrix} e^{jn\omega t} = j\frac{\rho c^2}{n\omega} \begin{Bmatrix} -Q_1/V_3 \\ (Q_2/V_7)\, e^{jn\phi} \end{Bmatrix} e^{jn\omega t}. \tag{12e}$$

For the eigenvalue solution,

$$|[K] - [M]\alpha^2| = 0. \tag{13}$$

Equation (13) has two distinct real and positive roots. The natural frequency expressions are tabulated in Table 1. The mode shapes $\{u\}_r$ are, for the first mode,

$$\{u\}_1 = \begin{Bmatrix} 1 \\ \dfrac{K_3 + K_5 - M_4\omega_1^2}{K_5} \end{Bmatrix} = \begin{Bmatrix} 1 \\ \dfrac{K_5}{K_7 + K_5 - M_6\omega_1^2} \end{Bmatrix}$$

$$= \begin{Bmatrix} 1 \\ 1 + \dfrac{V_5}{V_3} - \dfrac{V_5 l_4 \omega_1^2}{S_4 c^2} \end{Bmatrix} = \begin{Bmatrix} 1 \\ \dfrac{1}{1 + \dfrac{V_5}{V_7} - \dfrac{l_6 V_5 \omega_1^2}{S_6 c^2}} \end{Bmatrix}, \tag{14a}$$

TABLE 1

Natural frequencies of discharge system shown in Figure 1 in terms of both the mechanical analog (upper expressions) and the manifold parameters (lower expressions)

Natural frequency	
ω_1 first natural frequency	$\sqrt{\frac{1}{2}\left(\frac{K_3+K_5}{M_4}+\frac{K_7+K_5}{M_6}-\sqrt{\left(\frac{K_3+K_5}{M_4}-\frac{K_7+K_5}{M_6}\right)^2+\frac{4K_5^2}{M_4M_6}}\right)}$ $c\sqrt{\frac{1}{2}\left(\frac{S_4(V_5+V_3)}{l_4V_3V_5}+\frac{S_6(V_7+V_5)}{l_6V_7V_5}-\sqrt{\left\{\frac{S_4(V_5+V_3)}{l_4V_3V_5}-\frac{S_6(V_7+V_5)}{l_6V_7V_5}\right\}^2+\frac{4S_4S_6}{l_4l_6V_5^2}}\right)}$
ω_2 second natural frequency	$\sqrt{\frac{1}{2}\left(\frac{K_3+K_5}{M_4}+\frac{K_7+K_5}{M_6}+\sqrt{\left(\frac{K_3+K_5}{M_4}-\frac{K_7+K_5}{M_6}\right)^2+\frac{4K_5^2}{M_4M_6}}\right)}$ $c\sqrt{\frac{1}{2}\left(\frac{S_4(V_5+V_3)}{l_4V_3V_5}+\frac{S_6(V_7+V_5)}{l_6V_7V_5}+\sqrt{\left\{\frac{S_4(V_5+V_3)}{l_4V_3V_5}-\frac{S_6(V_7+V_5)}{l_6V_7V_5}\right\}^2+\frac{4S_4S_6}{l_4l_6V_5^2}}\right)}$

and, for the second mode,

$$\{u\}_2 = \begin{Bmatrix} 1 \\ \dfrac{K_3+K_5-M_4\omega_2^2}{K_5} \end{Bmatrix} = \begin{Bmatrix} 1 \\ \dfrac{K_5}{K_7+K_5-M_6\omega_2^2} \end{Bmatrix}$$

$$= \begin{Bmatrix} 1 \\ 1+\dfrac{V_5}{V_3}-\dfrac{V_5 l_4\omega_2^2}{S_4c^2} \end{Bmatrix} = \begin{Bmatrix} 1 \\ \dfrac{1}{1+\dfrac{V_5}{V_7}-\dfrac{l_6V_5\omega_2^2}{S_6c^2}} \end{Bmatrix}. \tag{14b}$$

3.2. FORCED ACOUSTIC OSCILLATIONS RESPONSE

The overall solution can be obtained by a superposition of the solutions due to both forcing functions. Consider

$$\{F\} = \begin{Bmatrix} F_1 \\ 0 \end{Bmatrix} e^{jn\omega t}. \tag{15}$$

Using equations (11), one obtains

$$h_r(t) = \frac{u_{1r}F_1}{\delta_r\{u\}_r^T[M]\{u\}_r}\left[\frac{\delta_r e^{jn\omega t}-(\eta_r+jn\omega)e^{-\eta_i t}\sin(\delta_r t)-\delta_r e^{-\eta_r t}\cos(\delta_r^t)}{(\eta_r^2+jn\omega)^2+\delta_r^2}\right]. \tag{16}$$

The terms involving $(\eta_r+j\omega)\sin(\delta_r t)$ and $\delta_r\cos(\delta_r t)$ can be ignored as they decay with time. Thus the total solution due to one forcing function $F_1 e^{j\omega t}$ is

$$\{X(t)\}_{F_1} = \sum_{r=1,2}\{u\}_r u_{1r}F_1\frac{1}{\{u\}_r^T[M]\{u\}_r}\cdot\frac{(1/\omega_r^2)e^{jn\omega t}}{\{[1-(n\omega/\omega_r)^2]+j2\xi_r(n\omega/\omega_r)\}}. \tag{17}$$

The overall solution of the volume displacement matrix is

$$\{X(t)\} = \{X(t)\}_{F_1} + \{X(t)\}_{F_2}, \tag{18}$$

or

$$\{X(t)\} = \sum_{r=1,2} \frac{\{u\}_r u_{1r}}{\{u\}_r^T [M] \{u\}_r} \frac{\rho c^2 Q_1}{n\omega V_3 \omega_r^2} \frac{e^{jn\omega t} e^{j[-(\pi/2)-\psi_r(n\omega)]}}{\sqrt{[1-(n\omega/\omega_r)^2]^2 + [2\xi_r(n\omega/\omega_r)]^2}}$$

$$+ \sum_{r=1,2} \frac{\{u\}_r u_{2r}}{\{u\}_r^T [M] \{u\}_r} \frac{\rho c^2 Q_2}{n\omega V_7 \omega_r^2} \frac{e^{jn\omega t} e^{j[(\pi/2)-\psi_r(n\omega)]} e^{jn\phi}}{\sqrt{[1-(n\omega/\omega_r)^2]^2 + [2\xi_r(n\omega/\omega_r)]^2}}, \quad (19a)$$

where

$$\psi_r(n\omega) = \arctan\{2\xi_r(n\omega/\omega_r)/[1-(n\omega/\omega_r)^2]\}. \quad (19b)$$

Equation (19) could be evaluated for each harmonic (n) and the final solution in the time domain could then be obtained by Fourier synthesis.

3.3. SYMMETRICAL SYSTEM

Very often a two-cylinder compressor has a symmetrical discharge system: i.e., with reference to Figure 1,

$$K_3 = K_7, \quad V_3 = V_7, \quad M_4 = M_6, \quad l_4 = l_6, \quad R_4 = R_6, \quad S_4 = S_6,$$
$$Q_1 = Q_2 = Q. \quad (20)$$

TABLE 2

Natural frequencies and mode shapes of a symmetrical discharge system (refer to Figure 5)

r	Mode	Natural frequency ω_r	Mode shape $\{u\}_r$
1	First	$c\sqrt{S_4/l_4 V_3}$	$\begin{Bmatrix} 1 \\ 1 \end{Bmatrix}$ Sloshing
2	Second	$c\sqrt{S_4/l_4[(1/V_3)+(2/V_5)]}$	$\begin{Bmatrix} 1 \\ -1 \end{Bmatrix}$ Compressive

The natural frequencies and mode shapes of a symmetrical case are listed in Table 2. The sloshing and compressive modes of gas oscillations are illustrated in Figure 3. The concept of a sloshing mode is that both fluid plugs (in necks #4 and #6) move as a unit, and that is why no

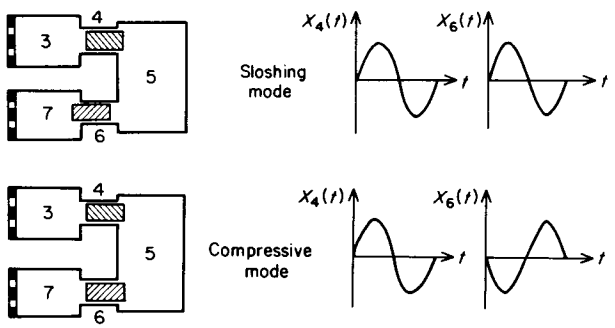

Figure 3. Modes of gas oscillations in a symmetrical two-cylinder compressor discharge manifold.

pressure fluctuations will be witnessed in the collector (#5). On the other hand, for a compressive mode, both fluid necks (#4 and #6) move opposite to each other: i.e., towards each other during half a cycle and away from each other during the other half.

3.4. EFFECT OF KINEMATIC PHASING ON RESPONSE

It is appropriate now to consider the following three cases for the nth harmonic: (a) $n\phi = 0$; (b) $n\phi = \pi$; (c) $n\phi$, but $n\phi \neq 0, \pi$. In equation (19a), it is convenient to introduce the notation

$$W_r = \frac{\{u\}_r}{\{u\}_r^T [M] \{u\}_r} \frac{\rho c^2 Q}{n\omega V_3 \omega_r^2} \frac{e^{jn\omega t} e^{-j\psi_r(n\omega)}}{\sqrt{[1-(n\omega/\omega_r)^2]^2 + [2\xi_r(n\omega/\omega_r)]^2}}, \qquad r = 1, 2, \tag{21}$$

where r represents the mode number. Equation (19) can be written for a symmetrical case ($Q_1 = Q_2 = Q$) as,

$$\{X(t)\} = W_1 u_{11} e^{-j(\pi/2)} + W_2 u_{12} e^{-j(\pi/2)} + W_1 u_{21} e^{j(\pi/2)} e^{jn\phi} + W_2 u_{22} e^{j(\pi/2)} e^{jn\phi}. \tag{22}$$

Since mode shapes for a symmetrical case are

$$u_{11} = 1, \qquad u_{12} = 1, \qquad u_{21} = 1, \qquad u_{22} = -1, \tag{23}$$

one obtains

$$\begin{aligned} \{X(t)\} &= W_1 e^{-j(\pi/2)} + W_2 e^{-j(\pi/2)} + W_1 e^{j(\pi/2)} e^{jn\phi} - W_2 e^{j(\pi/2)} e^{jn\phi} \\ &= W_1 [e^{-j(\pi/2)} + e^{j(n\phi + \pi/2)}] + W_2 [e^{-j(\pi/2)} - e^{j(n\phi + \pi/2)}]. \end{aligned} \tag{24}$$

For case (a), $n\phi = 0$,

$$\{X(t)\} = W_2(-2j \sin \pi/2) = -2jW_2. \tag{25}$$

Thus, those nth harmonics which are in phase with each other excite only a compressive ($r = 2$) mode.

For case (b), $n\phi = \pi$,

$$\{X(t)\} = W_1(e^{-j(\pi/2)} + e^{j(3\pi/2)}) + W_2(e^{-j(\pi/2)} - e^{j(3\pi/2)}) = -2jW_1. \tag{26}$$

Thus, those nth harmonics which are totally out of phase with each other excite only a sloshing ($r = 1$) mode.

For case (c) those harmonics whose phase difference is neither 0 nor π excite a combination of the sloshing and compressive modes.

The results for the above three cases are tabulated in Table 3. For a 180° kinematic phasing (ϕ) between the cylinder, odd harmonics excite only a sloshing mode, and even harmonics excite only a compressive mode.

TABLE 3

Effect of nth harmonics' phasing on symmetrical discharge system response

Phase	System response
0°	Only compressible mode excited
180°	Only sloshing mode excited
In between 0° and 180°	A combination of compressive and sloshing modes excited

4. RESULTS

4.1. EXAMPLE CASE

Table 4 illustrates the pertinent values of the example case. Note that l_4 and l_6, as listed in Table 4, are actual geometrical lengths; standard end corrections will have to be added to these for computations [13, 14].

TABLE 4
Example case

Number of cylinders m	2
Crank phasing ϕ	180°
Running speed f	59·66 Hz
„ „ ω	374·89 rad/s
Fluid medium	R-12 [CCl_2F_2]
Speed of sound c	169·2 m/s
Nominal discharge pressure	1·261 MPa
Nominal discharge temperature	73·3°C
V_3	$6{\cdot}194 \times 10^{-5}$ m^3
l_4	$3{\cdot}022 \times 10^{-2}$ m
S_4	$1{\cdot}225 \times 10^{-4}$ m^2
V_5	$9{\cdot}948 \times 10^{-5}$ m^3
l_6	$3{\cdot}022 \times 10^{-2}$ m
S_6	$1{\cdot}225 \times 10^{-4}$ m^2
V_7	$6{\cdot}194 \times 10^{-5}$ m^3

4.2. EIGENVALUE SOLUTION

Figure 4 shows the measured acoustic pressure response of the discharge plenum. A comparison of the natural frequencies of the internal discharge system is shown in Table 5. For measured frequencies, the uncertainty range is approximately ± 5 Hz.

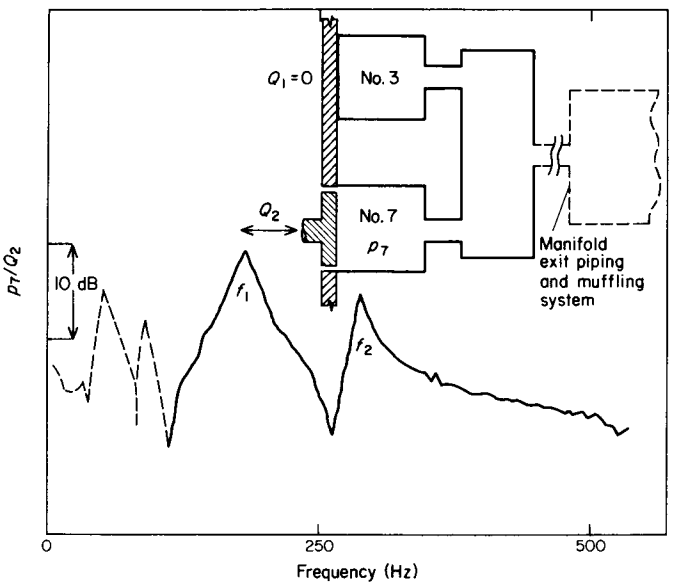

Figure 4. Measured acoustic pressure response of the discharge plenum (#7). This plenum was acoustically excited by a piston mounted on an electrodynamic shaker; the other discharge opening was blocked by a metal plate. Simultaneous acquisition and processing of microphone (p_7) and piston displacement transducer (Q_2) signals yielded the above transfer function [12]. The dotted portion of the curve, in the frequency range of interest, corresponds to the manifold exit piping and downstream muffling system. Fluid medium: R-12, zero mean flow.

TABLE 5

Comparison of acoustic natural frequencies

	Computed (Hz)	Measured (Hz)
f_1	190	190
f_2	284	285

Now the question arises: what about the exit piping and muffling system? If the components belonging to one of the cylinders are deleted, then the system is reduced to a single cylinder manifold. It now consists of a discharge plenum, connecting passage, half of the collector and the muffling system. Measurements (Figure 4) show that there are essentially two dominant low frequency resonances, one at 50 Hz and the other at 90 Hz. These are due to the gas oscillations in the components through which mean flow from one compressor would pass. The 190 Hz and 285 Hz resonances are due to the dynamic interactions between cylinders, which is of interest here. Also, these are of more significance than the lower frequency resonances.

4.3. FORCED OSCILLATION RESPONSE

The forced oscillation response of the example manifold can now be examined by using expressions (25) and (26). Since the kinematic phasing (ϕ) is 180°, odd harmonics would excite the sloshing mode; and even harmonics would excite the compressive mode. The overall volume displacement $X(t)$ is given by the sum of each harmonic's response:

$$\{X(t)\} = \sum_{\text{odd } n} \{X(t)\}_n + \sum_{\text{even } n} \{X(t)\}_n. \tag{27}$$

Using expressions (25) and (26) gives

$$\{X(t)\} = \sum_{\text{odd } n} (-2\mathrm{j}W_1)_n + \sum_{\text{even } n} (-2\mathrm{j}W_2)_n. \tag{28}$$

The fundamental frequency is 60 Hz and the odd harmonics are 60, 180, 300, ..., Hz, and even harmonics are 120, 240, 360, ..., Hz. The sloshing mode frequency is the only one which is close to an excitation frequency. Thus, the participation factors for all other excitations will be smaller (for an undamped case) than the sloshing mode and third harmonic combination. For $\xi_r = 0$,

$$\begin{aligned} (W_1)_{n=3} &\gg (W_1)_n, \quad \text{odd } n, n \neq 3, \\ &\gg (W_2)_n, \quad \text{even } n. \end{aligned} \tag{29}$$

Therefore,

$$\{X(t)\} \approx -2\mathrm{j}(W_1)_3. \tag{30}$$

Thus, for small damping, the response is mainly due to the sloshing mode. This can be verified by comparing it to the measurements as described in section 4.5.

4.4. COMPUTATION OF PLENUM PRESSURE

The fluctuating pressure in any element can be computed from the $X(n\omega)$ solution. For example, the plenum pressure $p_3(n\omega)$, or $p_7(n\omega)$, is

$$p_3(n\omega) = K_3[Q(n\omega) - X(n\omega)] = K_3[(1/\rho)\dot{m}(n\omega) - X(n\omega)]. \tag{31}$$

The mass flow rate data $\dot{m}(n\omega)$ has to be either known or assumed appropriately. For our case, a single cylinder computer simulation program was run with the discharge plenum V_3, or V_7, directly connected to an anechoic tube of 11 mm diameter [10, 20]. The simulation yielded the $\dot{m}(n\omega)$ data, as documented in Table 6. Although it cannot be considered to be very accurate, it is not influenced by the dynamic interactions between cylinders.

TABLE 6

Mass flow rate data

n	$\dot{m}(n\omega)$ (kg/s)
1	0·0794
2	0·0726
3	0·0626
4	0·0453
5	0·0317
6	0·0181
7	0·0045
8	0·0090
9	0·0159
10	0·0204

The damping coefficients, as given by equation (11g) with $\zeta = 150$, were computed for each mode and at each harmonic, i.e., excitation frequency. Some typical values are $\xi_1(3\omega) = 0{\cdot}631$, $\xi_2(4\omega) = 0{\cdot}485$ and $\xi_1(5\omega) = 0{\cdot}814$. (For purely viscous and thermal dissipations at the tube walls ($\zeta = 1$), these values are very low, being $\xi_1(3\omega) = 0{\cdot}0042$, $\xi_2(4\omega) = 0{\cdot}0032$ and $\xi_1(5\omega) = 0{\cdot}0054$.)

4.5. COMPARISON OF RESULTS

The results of the lumped parameters model with non-linear damping are compared, in Figure 5, to the measurements, and to those of the distributed parameters model with identical damping treatment [20]. Note that while the lumped parameters model here includes only the internal discharge manifold system as shown by Figure 1, the measurements and the distributed parameters computations also include the manifold exit pipe and the muffling system which is terminated anechoically (for details, see reference [20]).

The lumped parameters model predicts the dominance of the third harmonic, which is confirmed by the measurements and the distributed parameters model results. The inclusion of the realistic damping model prevents the theoretically computed third harmonic pressures from growing boundlessly.

The analysis presented in this paper also predicts that compressive mode resonance cannot be excited by an odd harmonic (the fifth in the present case). This is verified by good agreement with the distributed parameters model results. However, the measurements show a small resonance peak at the fifth harmonic. This could be due to the lack of complete symmetry in the actual compressor where measurements were performed. The manifold exit impedance also has some influence on the fifth harmonic prediction as both the measurements and the distributed parameters model results show similar trends.

The exclusion of the manifold exit impedance has clearly affected the prediction of the first (or possibly second?) harmonic as two minor resonances at 50 Hz and 90 Hz are not accounted for.

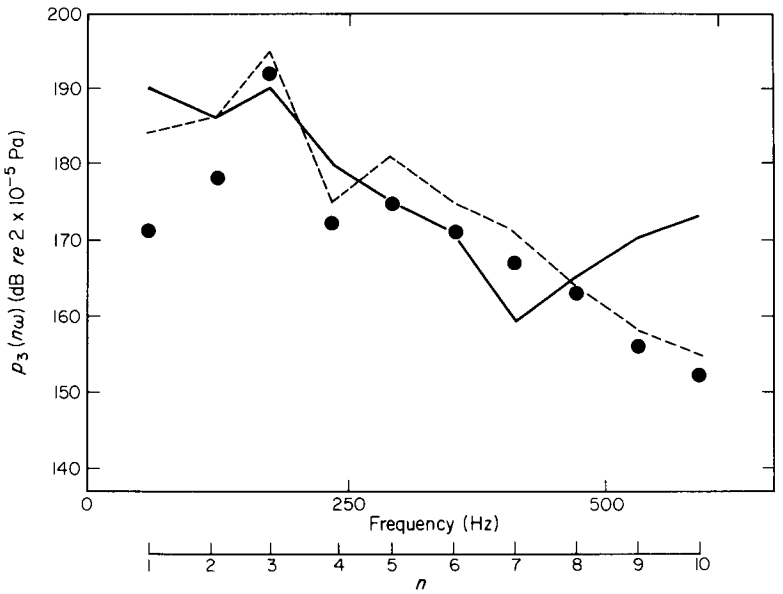

Figure 5. Discharge plenum pressure $p_3(n\omega)$. Harmonics of 59·66 Hz or 374·89 rad/s. ———, Computed by using lumped parameters model with non-linear damping; – – –, measured; ●, computed by using distributed parameters model with non-linear damping [20].

At higher frequencies, the lumped parameters model becomes inaccurate, as shown in Figure 5, where, after the seventh harmonic, the lumped parameters model results do not compare favorably with either the measurements or the distributed parameters model results.

It can be stated that the lumped parameters model predicts ' ell at low frequencies, especially in the frequency range of cylinder interactions. The agree ient with measurements is satisfactory in view of the simplifications and assumptions used in the analysis.

5. CONCLUDING REMARKS

The present study is different in character from previous investigations in which the lumped parameters approach was used for modeling and simulation purposes [2–5]. Here the intent has been to use it as a tool to supplement more detailed modeling efforts [10–12] in such a way that an insight into the dynamic behavior of the manifold interactions is obtained. The multicylinder problem was generalized and the dynamic response was expressed in terms of gas modes of oscillation. This modal expansion technique has long been an analytical tool in structural dynamics but is rarely seen in the discipline of unsteady fluid dynamics. It has been instrumental in bringing out the critical kinematic and geometrical design points.

The lumped parameters analysis is potentially powerful for analyzing practical manifolds. The distributed parameters analysis of such cases is difficult. Also, a good and sound physical understanding of the system dynamics is obtained. As is true for all dynamic systems, the basic nature of a complicated acoustic system can be understood better and explained easily (and maybe effectively) if it is reduced to a simple system: i.e., in one or two degrees of freedom format. Amongst the limitations of a lumped parameters approach, the most severe is that it is sometimes not possible to identify the fluid masses and springs. At times there may not be any valid reason to assume that a particular inertial element has no elastic effects at all, and vice versa. An ideal solution would be to discretize a system more and more until all of the effects have been accounted for or to use Rayleigh–Ritz type elemental descriptions.

REFERENCES

1. R. SINGH and W. SOEDEL 1974 *Proceedings of the 2nd Purdue Compressor Technology Conference, West Lafayette, Indiana*, 102–123. A review of compressor lines pulsation analysis and muffler design research, Part I—Pulsation effects and muffler criteria, Part II—Analysis of pulsating effects.
2. W. SOEDEL, E. PADILLA NAVAS and B. B. KOTALIK 1973 *Journal of Sound and Vibration* **30**, 263–277. On Helmholtz resonator effects in the discharge system of a two-cylinder compressor.
3. W. SOEDEL 1972 *Proceedings of the 2nd Purdue Compressor Technology Conference, West Lafayette, Indiana*, 136–139. On the simulation of anechoic pipes Helmholtz resonator models of compressor discharge systems.
4. W. SOEDEL and J. M. BAUM 1976 *Proceedings of the 3rd Purdue Compressor Technology Conference, West Lafayette, Indiana*, 257–270. Natural frequencies and modes of gases in multicylinder compressor manifolds and their use in design.
5. B. R. C. MUTYALA and W. SOEDEL 1976 *Journal of Sound and Vibration* **44**, 479–491. A mathematical model of Helmholtz resonator type gas oscillation discharges of two-stroke cycle engines.
6. D. KARNOPP 1975 *Journal of Sound and Vibration* **42**, 437–446. Lumped parameter models of acoustic filters using normal modes and bond graphs.
7. D. SCHWERZLER 1971 *Ph.D. Thesis, Purdue University*. Mathematical modeling of multiple cylinder refrigeration compressor.
8. W. M. WANG 1967 *Journal of the Acoustical Society of America* **42**, 1244–1249. Acoustical analysis of a multicylinder engine air-induction system.
9. R. S. BENSON and A. S. UCER 1973 *Journal of Mechanical Engineering Science* **15**, 34–37. A theoretical pulsation in pipe systems with multiple reciprocating air compressors and receivers.
10. R. SINGH, E. SANDGREN, K. RAGSDELL and W. SOEDEL 1976 *American Society of Mechanical Engineers Winter Annual Meeting, ASME Paper No. 76-WA/FE-10*. Simulation of a two cylinder compressor for discharge gas oscillation prediction.
11. R. SINGH 1975 *Ph.D. Thesis, Purdue University*. Modeling of multicylinder compressor discharge systems.
12. R. SINGH and W. SOEDEL 1978 *Journal of Sound and Vibration* **56**, 105–125. An efficient method of measuring impedances of fluid machinery manifolds.
13. S. N. RSCHEVKIN 1963 *A Course of Lectures on the Theory of Sound*. New York: McMillan Company.
14. P. M. MORSE and K. U. INGARD 1968 *Theoretical Acoustics*. New York: McGraw-Hill Book Company.
15. T. R. STALZER and G. J. FIELDER 1956 *ASME 56-IRD-21*. Criteria of validity of lumped parameter representation of ducting air flow characteristics.
16. M. ALSTER 1972 *Journal of Sound and Vibration* **24**, 63–85. Improved calculation of resonant frequencies of Helmholtz resonators.
17. R. SINGH and W. SOEDEL 1978 *Journal of Sound and Vibration* **57**, 449–452. Assessment of fluid induced damping in refrigeration machinery manifolds.
18. W. SOEDEL 1975 *Conference on Vibration and Noise in Pump, Fan and Compressor Installations, University of Southampton, Paper No. 29*. On discretized modeling of flow pulsations in multicylinder gas machinery manifolds.
19. L. MEIROVITCH 1967 *Analytical Methods in Vibrations*. New York: McMillan Company.
20. R. SINGH and W. SOEDEL 1979 *Journal of Sound and Vibration* **63**, 125–143. Mathematical modeling of multicylinder compressor discharge system interactions.

APPENDIX A: ASSESSMENT OF ACOUSTIC DAMPING

The acoustic pressure $p(x, t)$ for a plane wave is

$$p(x,t) = \{A_+ e^{-\alpha x} e^{-j\omega x/c} + A_- e^{\alpha x} e^{j\omega x/c}\} e^{j\omega t}, \tag{A1}$$

where A_+ and A_- are amplitudes of the right-hand and left-hand travelling waves, respectively, x is the longitudinal co-ordinate, and α is the damping factor which

characterizes the wave attenuation per unit path length. For viscous and thermal dissipations at the walls of a tube of unit length and cross-sectional area S,

$$\alpha_\mu = (\pi\mu\omega/2S\rho c^2)^{1/2}. \tag{A2}$$

Note that α_μ is numerically small except for long and narrow tubes, and at high frequencies.

In order to model the overall damping, including fluid-induced effects, the measured damping factor α is assumed to be proportional to α_μ:

$$\alpha = \zeta\alpha_\mu. \tag{A3}$$

Here ζ is an empirical non-dimensional constant. In the absence of mean fluid flow, $\zeta = 1$ (i.e., $\alpha = \alpha_\mu$) has been found to be adequate for modeling purposes [12]. However, in an operating compressor with an R-12 fluid medium and with a gas velocity approximately corresponding to a Mach number of 0·1, ζ is approximately equal to 150. The acoustic wave equation in the lumped parameters format is

$$M\ddot{X}(t) + R\dot{X}(t) + KX(t) = 0, \tag{A4}$$

where R is the acoustic damping and is given by, for a tube of length l and cross-sectional area S [13],

$$R = r_1 l/S, \tag{A5}$$

where r_1 is the coefficient of friction per unit length and per unit area of the tube. From reference [13], the relationship between r_1 and α is

$$r_1 = 2\rho c\alpha. \tag{A6}$$

Thus for a tube of length l and cross-sectional area S,

$$R = 2\rho c\zeta\alpha_\mu l/S = (2\pi\zeta^2\mu\omega/\rho S)^{1/2}(\rho l/S) = (2\pi\zeta^2\mu\omega/\rho S)^{1/2}M. \tag{A7}$$

APPENDIX B: NOMENCLATURE

c speed of sound
f frequency
F forcing function
j imaginary unit ($=\sqrt{-1}$)
K acoustic stiffness
l length
m number of cylinders
$\dot{m}_v$ mass flow rate
M acoustic mass
n harmonic number
p acoustic pressure
P total number of modes
Q input volume velocity
R acoustic damping
S cross-sectional area
t time
u mode shape
$X, \dot{X}, \ddot{X}$ acoustic volume displacement, velocity and acceleration
μ fluid viscosity
δ modal damped natural frequency
θ crank angle
ξ modal damping factor
ϕ crank phasing between cylinders
ψ phase of a complex quantity
ω frequency (rad/s)
ζ fluid-induced damping coefficient

Subscripts

1 cylinder no. 1, valve exit of cylinder no. 1
2 cylinder no. 2, valve exit of cylinder no. 2
n nth harmonic
r rth mode